A Malignant Melanoma Imaging Agent: Synthesis, Characterization, In Vitro Binding and Biodistribution of Iodine-125-(2-Piperidinylaminoethyl)4-Iodobenzamide

C.S. John, W.D. Bowen, T. Saga, S. Kinuya, B.J. Vilner, J. Baumgold, C.H. Paik, R.C. Reba*, R.D. Neumann, V.M. Varma and J.G. McAfee

The George Washington University Medical Center, Washington, DC; Laboratory of Medicinal Chemistry, National Institute of Diabetes and Digestive and Kidney Diseases and Nuclear Medicine, National Institutes of Health, Bethesda, Maryland

In order to develop improved radiopharmaceuticals for imaging malignant melanoma, we have synthesized and characterized ^{125}I- and ^{131}I-labeled (2-piperidinylaminoethyl)4-iodobenzamide (PAB). In vitro binding profiles of IPAB and N-(2-diethylaminoethyl)4-iodobenzamide (IDAB, a structurally related analog of IPAB) for a variety of neurotransmitter receptors suggested that both IPAB and IDAB possessed a high sigma-1 affinity and a low affinity for sigma-2 sites. In vitro homologous competition binding studies of [^{125}I]PAB with human malignant melanoma cell A2058 showed that the tracer was bound to the cells with a high affinity (Ki = 6.0 n*M*) and that the binding was saturable. Biodistribution studies in nude mice implanted with human malignant melanoma xenografts showed good tumor uptake (3.87% ID/g at 1 hr, 2.91% ID/g at 6 hr and 1.02% ID/g at 24 hr) of [^{125}I]PAB. High tumor-to-nontarget organ ratios were obtained at 24 hr postinjection. Tumor-to-blood, liver, muscle, lung, intestines, heart and brain ratios at 24 hr were 17.80, 3.88, 94.58, 14.29, 10.87, 37.07 and 90.01, respectively. Tumor imaging with [^{131}I]PAB in a nude mice model xenografted with human malignant melanoma at 24 hr clearly delineated the tumor with very little activity in any other organ. These results demonstrate that sigma-1 receptors could be used as external markers for malignant melanoma.

J Nucl Med 1993; 34:2169–2175

Malignant melanoma is a common tumor and its frequency is increasing in the general population. The mortality rate worldwide has doubled over the past 20 yr. A recent NIH consensus panel concluded that 7200 new cases of melanoma are expected to be diagnosed this year and about 2400 deaths related to this disease are expected in 1992 (*1*).

Received Apr. 6, 1993; revision accepted Aug. 5, 1993.

For correspondence or reprints contact: Christy S. John, PhD, Radiopharmaceutical Chemistry Section, 662 Ross Hall, 2300 I St. NW, Washington, DC 20037.

*Present address: University of Chicago Hospitals, Nuclear Medicine Section, 5841 S. Maryland Ave., Chicago, IL 60637.

Radiolabeled monoclonal antibodies or their fragments that bind to specific melanoma antigens have been recently tried for localizing malignant melanoma. In clinical trials at multiple centers, limited success has been reported so far (*2–8*). A variety of other radiopharmaceuticals have been evaluated for the scintigraphic detection of malignant melanoma. These include iodinated chloroquine analogs (*9–12*) and 5-iodo-2-thiouracil (*13*) derivatives. It has been proposed that these compounds possess some melanotropic affinity and are therefore incorporated into the melanin pigment of melanoma. However, the successful use of these radiopharmaceuticals in human beings has not been reported. Iodine-123-N-isopropyl p-iodoamphetamine (IMP), a new brain imaging agent, has demonstrated metastatic melanoma in three of four patients (*14*). Cohen and coworkers reported the use of [^{123}]IMP in the detection of primary and metastatic malignant melanoma (*15*).

More recently, Michelot et al. (*16*) described another radiopharmaceutical [^{125}I]N-(2-diethylaminoethyl)-4-iodobenzamide (IDAB) for the detection and therapy of malignant melanoma. In comparison, [^{125}I]IMP had a slower blood clearance and its uptake in other organs such as liver, lung, brain and muscle was higher than that of tumor at 24 hr. Hence, good images could not be obtained because of low contrast. It was therefore concluded that IDAB was a better tracer than IMP for imaging malignant melanoma. In clinical trials in Europe, [^{123}I]DAB has been successfully used in the diagnosis of malignant melanoma (*17*).

One of the problems with IDAB was the method of radioiodination. In the original report (*16*), it was synthesized from N-(2-diethylaminoethyl)4-aminobenzamide. This amino compound was diazotized with sodium nitrite and hydrochloric acid and then treated with potassium iodide and sodium iodide (^{125}I). The yield of [^{125}I]DAB was 45% and a low specific activity (2.3 mCi/mmol) of the product was obtained. Iodination also was attempted by an isotopic exchange method. In this procedure, cold IDAB

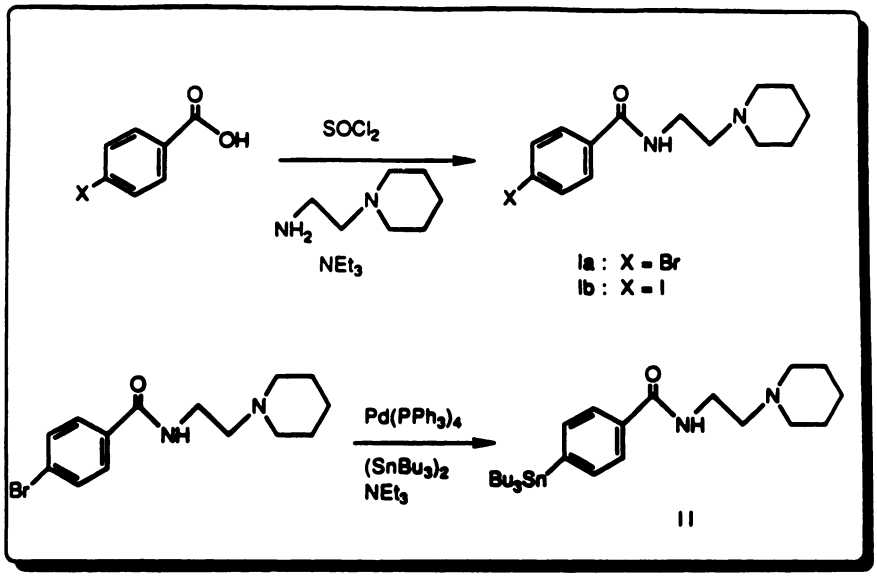

SCHEME 1.
Preparation of tributyltin PAB.

was heated with $Na^{125}I$ at 150°C for 35 min in the presence of copper sulfate as a catalyst. The iodinated product using this method also had low specific activity (36 mCi/mmol).

We recently reported an improved synthesis of [^{125}I]DAB from the precursor N-(2-diethylaminoethyl)4-tributyltinbenzamide in high yield and high specific activity (*18*). The biodistribution of [^{125}I]DAB in nude mice with human melanoma xenografts indicated a high uptake of the radiopharmaceutical in nontarget organs such as the liver and lung and a slow clearance from these organs. In an attempt to prepare new radiopharmaceuticals with high tumor uptake and low nontarget organ uptake and to understand the mechanism of uptake and retention of these benzamides, we report the synthesis, characterization, in vitro binding to sigma receptors and biological evaluation of N-(2-piperidinylaminoethyl)4-iodobenzamide (IPAB) (*19*) as a radiopharmaceutical for imaging malignant melanoma.

MATERIALS AND METHODS

Melting points were determined with a Fisher-Johns apparatus and are reported uncorrected. Proton and ^{13}C NMR spectra were recorded on a Bruker 300 AM spectrometer. Unless noted, chemical shifts were expressed as ppm using tetramethylsilane as an internal standard. All chemicals were obtained from Aldrich Chemical Company, Milwaukee, WI. The thin-layer chromatography (TLC) system consisted of Analtech uniplate silica gel GF plates (250 microns, 10 × 20 cm) developed with $CHCl_3$/MeOH: 80/20. Radioactive spots were scanned and recorded by a Bioscan 300 imaging scanner equipped with automatic plate reader. Mass spectra (chemical ionization) were recorded on a Finnigan 1015 mass spectrometer. $Na^{131}I$ was obtained from duPont NEN, and $Na^{125}I$ was obtained from Bristol Myers Squibb. Elemental analyses were performed by Galbraith Laboratory of Knoxville, TN.

Chemistry

Preparation of (2-piperidinylaminoethyl)4-bromobenzamide Ia (Scheme 1). A round-bottom flask was charged with 4-bromobenzoic acid (2.0 g, 9.95 mmol) in chloroform (150 ml). To the solution was added thionyl chloride (3 ml) in chloroform (10 ml), 2–3 drops of DMF; the slurry was heated at reflux for 3 hr as the reaction was monitored through a bubbler. A clear solution of 4-bromobenzoyl chloride was obtained, the volatiles were removed and a light yellow oil was obtained that solidified upon cooling. The acid chloride was dissolved in chloroform (30 ml) and added to another flask containing 1-(2-aminoethyl)piperidine (1.29 g, 10 mmol) in chloroform (20 ml) and triethylamine (10 ml) was added dropwise. The mixture was stirred at room temperature for 1 hr and the volatiles were removed in vacuo. The resulting slurry was washed with 2% sodium bicarbonate (2× 50 ml). The organics were dissolved in $CHCl_3$ (100 ml), separated from the aqueous layer and dried over anhydrous Na_2SO_4; the solvent was removed to give a colorless solid (2.7 g, yield, 87%). Rf ($CHCl_3$/MeOH:90/10) 0.45. ^{1}H NMR (∂ ppm): 1.46 (t, 2 H, CH_2); 1.54 (broad m, 4 H, CH_2); 2.43 (broad s, 4H, NCH_2); 2.52–2.56 (t, 2 H, NCH_2); 3.49–3.53 (dt, 2 H, NCH_2); 7.21 (bs, 1 H, NH); 7.52–7.55 (m, 2 H, arom); 7.65–7.68 (m, 2 H, arom).

Preparation of (2-piperidinylaminoethyl)4-iodobenzamide, Ib. This was prepared using a procedure similar to the one above to give a white solid in 89% yield. ^{1}H NMR (∂ ppm): 1.43–1.45 (broad m, 2 H, NCH_2); 1.53–1.60 (broad m, 4 H, NCH_2); 2.41 (broad m, 4 H, NCH_2); 2.50–2.54 (t, 2 H, J = 7.8 Hz, NCH_2); 3.44–3.48 (dt, 2 H, NCH_2); 7.02 (bs, 1 H, NH); 7.47–7.49 (m, 2 H, arom.); 7.73–7.76 (m, 2 H, arom.). m.p. 114–115 C. Anal $C_{14}H_{19}N_2OI$ calcd. C, 46.91; H, 5.31; N, 7.82, found C, 46.91; H, 5.42; N, 7.68.

Preparation of (2-piperidinylaminoethyl)4-tributyltinbenzamide, II. A flame-dried flask was charged with 4-bromobenzamide 1a, (1.0 g, 3.21 mmol) in triethylamine (40 ml). To the flask were added tetrakis(triphenyl phosphine)palladium (370 mg, 0.321 mmol), and bistributyltin (2.4 g, 3.80 mmol) and the mixture was refluxed under nitrogen for 12 hr. The mixture was then cooled, the solvents decanted from the black residue, and the volatiles were removed in vacuo. The resulting black oil was passed through a silica gel column and eluted first with $CHCl_3$ (100 ml) and then $CHCl_3$/MeOH:90/10. The desired fractions were pooled and solvent was evaporated to give an oil (0.4 g, 56%). m/e = 523 (M^+ +H)(100%); 233 (M^+ $-SnBu_3$) (40%). ^{1}H NMR (∂ ppm): 0.82–0.93 (m, 16 H, Bu_3 and CH_2); 1.01–1.05 (m, 4 H, Bu_3); 1.22–1.37 (m, 8 H, Bu_3); 1.45–1.67 (m, 8 H, piperidinyl ring);

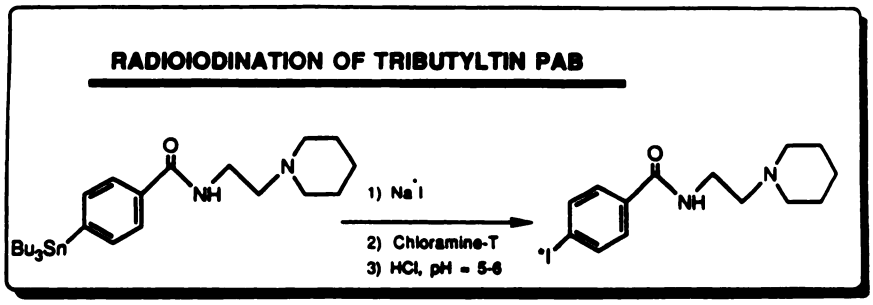

SCHEME 2.
Radioiodination of tributyltin PAB.

2.49–2.51 (t, 2 H, NCH_2 piperidinyl ring); 2.60–2.63 (t, 2 H, J = 6Hz, NCH_2); 3.53–3.58 (dt, 2 H, J = 5.34 Hz, NCH_2); 7.30–7.41 (bs, 1 H, NH); 7.49–7.78 (m, 4 H, arom). ^{13}C NMR (∂, ppm): 9.60, 13.58, 25.743, 27.30, 29.00, 36.09, 54.29, 57.15, 126.03, 128.39, 132.00, 136.54, 167.69.

Radiochemistry

Radiolabeling of n-tributyltin PAB with ^{125}I (Scheme 2). To 100 μl of an ethanolic solution of (2-piperidinylaminoethyl)4-tributyltinbenzamide (1 mg/ml) was added a solution of [^{125}I]NaI (1.5 mCi, 3 μl) in 0.1 N NaOH, followed by the addition of 0.05 N HCl (50 μl). The pH of the solution was between 4.5–6. Fifty microliters of a freshly prepared solution of N-chloro-4-toluenesulfonamide sodium monohydrate, chloramine-T (1 mg/ml) was added to the above mixture. The contents were stirred for 10–15 min at room temperature and 100 μl of a solution of sodium metabisulfite (200 mg/ml) were added.

The reaction mixture was neutralized with a saturated solution of $NaHCO_3$ (0.2 ml), after which 0.4 ml of normal saline was added and the organics were extracted in $CHCl_3$ (1.0 ml) after vortexing 30 sec. The chloroform layer was evaporated in a stream of nitrogen and the activity of the aqueous layer and the organic residue was counted. The total recovered activity in the residue ranged from 74% to 89% (n = 6). The residue was dissolved in 90% ethanol, and 10% 0.01 *M* phosphate buffer (400 μl), co-spotted with cold IPAB (synthesized as described in the chemistry section) on a TLC-SG plate and developed with $CHCl_3$/MeOH:90/10 (Rf = 0.45) and injected into a Gilson HPLC and fitted with a Waters Z-module radial compression separation system containing a micro BondaPak C-18 reverse-phase column equipped with Rheodyne 4125 injector (0.5 ml loop). The retention time for ^{125}I-PAB using isocratic elution with EtOH/0.01 *M* phosphate buffer (pH = 6.7):90/10, at a flow rate of 1 ml/min was found to be 8.5 min, a value identical to that of nonradioactive (2-piperidinylaminoethyl)4-iodobenzamide. Figure 1 shows HPLC traces of a crude reaction mixture for the preparation of [^{125}I] PAB.

Radiolabeling of n-tributyltin PAB with ^{131}I. The same protocol as above was used except that the amount of 0.05 N HCl added to adjust the pH between 4.5–6.0 varied due to different concentrations of aqueous sodium hydroxide present in the commercially supplied Na^{131}I. The workup of the reaction and its purification was identical to the above.

Cell Culture and Tumor Model

A2058 is a cell line derived from a brain metastasis of human malignant melanoma (*20*). These cells were grown in DMEM2 (Dulbecco's modification of Eagle's) medium supplemented with 10% fetal bovine serum and 0.03% L-glutamine. For in vivo studies, these cells were removed using calcium and magnesium-free PBS containing 0.02% EDTA. A suspension of 5×10^6 cells (viability greater than 95%) in 0.2 ml of medium were inoculated subcutaneously in female Balb/c nu/nu mice. After about 2 wk, the solid tumor grew to optimal size (about 1 cm in diameter) and was used for the biodistribution studies. Tumor formation occurred in 85% of the mice.

In Vitro Sigma-1 Binding Assay

To a set of numbered test tubes were added guinea pig brain membranes (300–500 μg protein) which were incubated with 3 n*M* [^{3}H]-(+)-pentazocine (51.7 Ci/mmol) in 0.5 ml of 50 m*M* Tris-HCl, pH 8.0, for 120 min at 25°C. IDAB and IPAB were added in concentrations ranging from 10^{-4} to 10^{-12} *M*. Assays were terminated by the addition of 5 ml ice-cold 10 m*M* Tris-HCl, pH 8.0, and filtered through glass fiber filters using a Brandel cell harvester (Gaithersburg, MD). The filters were then washed twice with 5 ml ice-cold 10 m*M* Tris-HCl, pH 8.0. Nonspecific binding was determined in the presence of 10 μ*M* (+)-pentazocine C6 glioma cell membranes (100 μg proteins) were incubated as described for guinea pig brain except that assays were carried out at 37°C using 30 n*M* [^{3}H](+)-pentazocine in a final volume of 0.25 ml. The filters were soaked in 0.5% polyethyleneimine prior to use. Scintillation counting was performed in an Ecoscint (National Diagnostics, Manville, NJ) after an overnight extraction of counts. Protein was determined by the Lowry method.

In Vitro Sigma-2 Binding Assay

Rat liver membranes (150–200 μg of protein) or C6 glioma cell membranes (100 μg protein) were incubated with 3 n*M* [^{3}H]DTG

TABLE 1
Sigma Binding Profiles of IPAB and IDAB

	Sigma-1 (Ki, n*M*) [^{3}H](+)-Pentazocine		Sigma-2 (Ki, n*M*) [^{3}H]DTG+dextrallorphan	
	Guinea pig brain	C6 glioma	Rat liver	C6 glioma
IDAB	11(±)3.93	6.86(±)1.95	2041(±)454	2900(±)488
IPAB	2.57(±)0.70	1.70(±)0.33	205(±)67	158(±)20

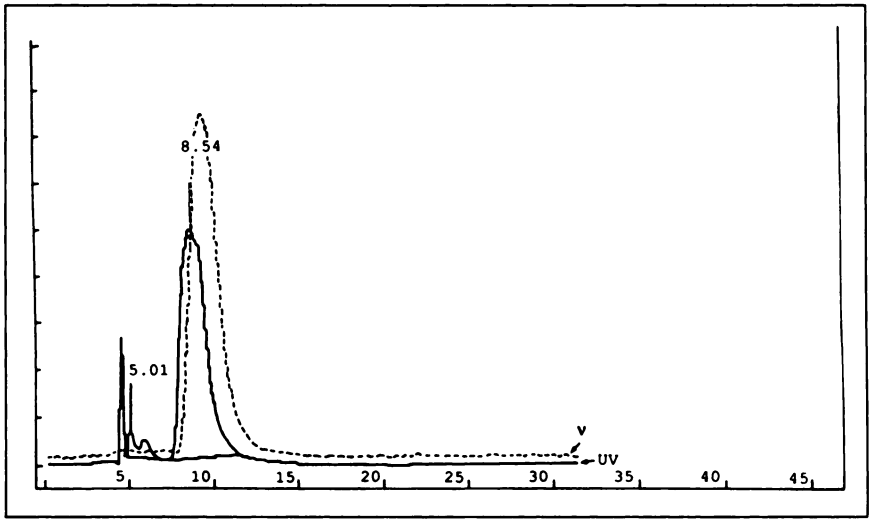

FIGURE 1. HPLC traces of crude reaction mixture for the preparation of [^{125}I]PAB.

(39.4 Ci/mmol) in the presence of 1 μM dextrallorphan (to mask sigma-1 sites) at 25°C for 120 min. The procedure was the same as above except that nonspecific binding was determined in the presence of 5 μM haloperidol. IC_{50} values for both the sigma-1 and sigma-2 assays were determined using the computerized iterative curve-fitting program GraphPAD (San Diego, CA). Ki values were calculated from IC_{50} values using the Cheng-Prusoff equation. Sigma binding profiles of IPAB and IDAB ligands are given in Table 1.

In Vitro Cell Binding Studies

Human malignant melanoma cells (A2058) were grown as described above. The cells were harvested with phosphate buffer (0.1 M) containing 0.02% EDTA without Ca^{+2} and Mg^{+2} ions. The cells were then washed twice with ice-cold RPMI 1640 medium (Gibco) without glutamine and resuspended in the same medium. A small volume (0.1 ml) containing 1.5 × 10^6 cells in eight sets of test tubes were incubated separately with carrier-free [^{125}I]PAB (0.1 ml) and varying concentrations of cold IPAB. The contents were incubated at 37°C for a period of 5 hr. At the end of this incubation, the cells were centrifuged for 5 min, the supernatant was discarded and the cells washed with RPMI 1640 medium and then counted. The data were analyzed with the iterative nonlinear least squares curve-fitting program INPLOT. The competition binding assay curve for [^{125}I]PAB is shown in Figure 2.

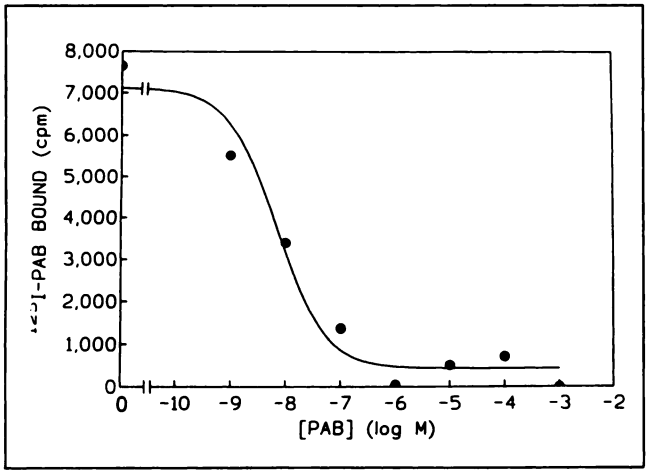

FIGURE 2. Homologous competition binding assay of [^{125}I]PAB to human malignant carcinoma (A2058) cells.

Animal Biodistribution Studies

Balb/c nu/nu mice (17–22 g) were injected intravenously with 0.2 ml of a saline solution containing [^{125}I]PAB (5–6 μCi). At 1, 6 and 24 hr after injection, blood samples were collected by cardiac puncture and the mice were killed immediately thereafter by cardiectomy while under halothane anesthesia. Six animals were studied at each time point. The organs of interest were subsequently excised, blotted with tissue paper, weighed and the radioactivity was counted using a Packard automatic counter (autogamma 5650). The percent injected dose per gram (%ID/g) values were determined by comparison of the tissue radioactivity with suitably diluted aliquots of the injected dose and divided by the weight of the organ. The values obtained were linearly normalized to a mouse weighing 20 g.

Nude Mice Imaging Studies

Balb/c nu/nu mice (17–22 g) bearing human melanoma xenografts were injected intravenously with 0.2 ml of a saline solution containing [^{131}I]PAB or [^{131}I]DAB (150–200 μCi). The animals were anesthetized with ketamine containing rompun before the imaging studies. Images were obtained using a scintigraphic camera with a pinhole collimator at 6 and 24 hr postinjection. Figure 2 shows the scintigrams of nude mice implanted with human melanoma xenografts obtained for [^{131}I]DAB and Figure 3 shows the scintigrams obtained for [^{131}I]PAB.

RESULTS AND DISCUSSION

In the present report, synthesis of PAB was achieved by conversion of 4-bromobenzoic acid to the 4-bromobenzoylchloride using thionyl chloride as a chlorinating agent in the presence of DMF as a catalyst. This acid chloride was condensed with 1(2-aminoethyl)-piperidine. The aqueous workup and purification by column chromatography provided pure (2-piperidinylaminoethyl)4-bromo-benzamide in a high yield (87%). The tri-n-butyltin precursor was synthesized using a published procedure of Clanton and coworkers (*21*). This debromostannylation reaction in-

volved the use of bromobenzamide, Ia, bis(tributyltin), one-tenth equivalent of tetrakis(triphenyl phosphine) palladium (0), and refluxing in dry triethylamine to give modest yields (56%) of tributyltin substituted benzamide as shown in Scheme 1. The compound was characterized by ^{1}H and ^{13}C NMR and mass spectroscopic analysis.

Iodine-125-PAB was prepared from the tributyltin derivative in high yields (78%–94%) and high specific activity by reaction with $Na^{125}I$ or $Na^{131}I$ in the presence of chloramine-T as an oxidizing agent. This synthesis is schematically shown in Scheme 2. The radiolabeled product was extracted in chloroform, and dissolved in 90% ethanol with 0.01 *M* phosphate buffer (400 μl) after the evaporation of chloroform under a stream of nitrogen gas. The product was HPLC purified.

Figure 1 shows the HPLC traces of a crude reaction mixture of [^{125}I]PAB (gamma) and IPAB (UV). The retention time of IPAB using ethanol/0.01 *M* phosphate buffer solution in a 90:10 ratio at a flow rate of 1.0 ml/min is 8.54 min. The retention time for IDAB under identical conditions is about 10 min. The radiochemical purity of the desired fraction was greater than 98%. Radiochemical yield and purity are so high that this protocol could be easily developed to a kit formulation. The coinjection of the authentic cold compound and tracer gave a single peak on HPLC. The specific activity of [^{125}I]PAB as determined by HPLC was high (>1800 Ci/mmol).

The iodobenzamides IPAB and IDAB were evaluated for their activity at sigma receptors (*22*) by competition in membranes of guinea pig brain, rat liver and C6 glioma cells. Sigma-1 sites were labeled with sigma-1 selective ligand, [^{3}H](+)-pentazocine, and sigma-2 sites were labeled with subtype nonselective ligand, [^{3}H]-1,3-di-tolylguanidine ([^{3}H]DTG). Both IPAB and IDAB bound with a high affinity to sigma-1 sites present in guinea pig brain and C6 glioma cell membranes and with a low affinity to sigma-2 subtype receptors present in C6 glioma cell and rat liver membranes. In vitro binding studies of [^{125}I]PAB to A2058 cells showed that binding was saturable and that the ligand was bound to the cells with a high affinity [Ki = 6.0 n*M*]. This result implies that radiolabeled iodobenzamides bind to the cell surface sigma-1 receptors on human malignant melanoma cells. Sigma receptors have also been reported to be present on some other tumor-derived cells (*23*). Both IPAB and IDAB had low affinity for D-2 dopaminergic sites.

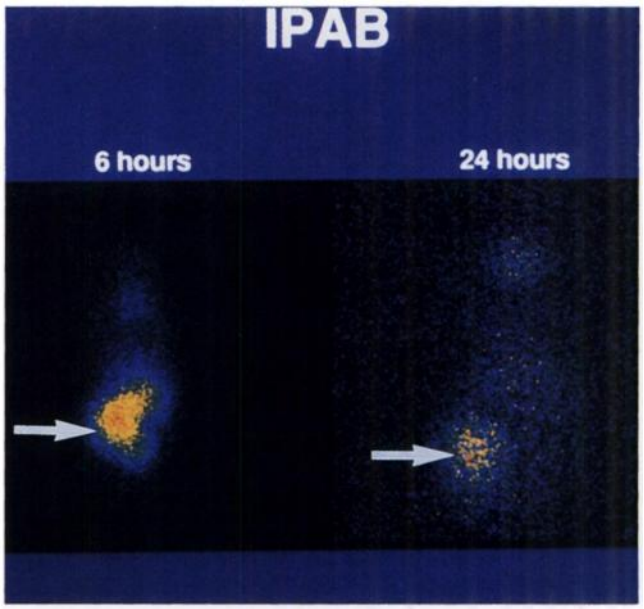

FIGURE 4. Scintigraphic images of nude mice bearing human malignant melanoma xenografts using [^{131}I]PAB. Arrows indicate implanted tumor site.

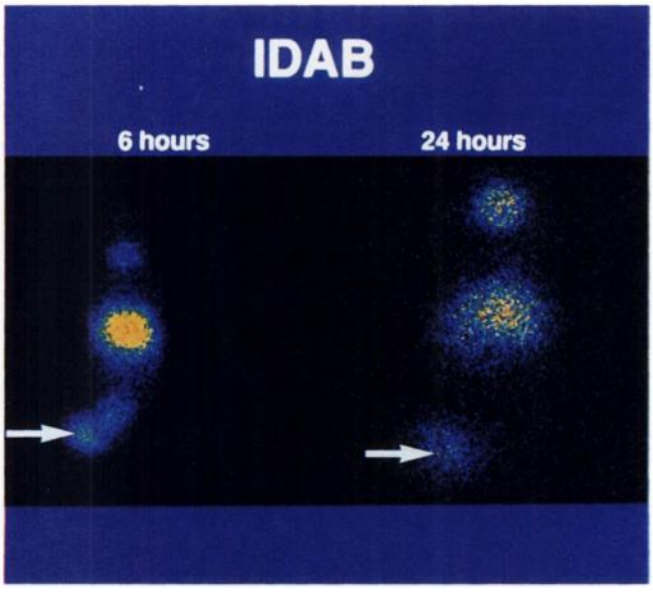

FIGURE 3. Scintigraphic images of nude mice bearing human malignant melanoma using [^{131}I]DAB. The arrow indicates the implanted tumor site.

The biodistribution of [^{125}I]PAB and [^{125}I]DAB is compared in nude mice bearing human melanoma xenografts in the flank in Tables 2–4 at 1, 6 and 24 hr, respectively. The differences between the two agents were examined by Student's unpaired t-tests. The tumor concentration (%ID/g) was higher with [^{125}I]DAB at 1 hr, but almost twice as high with [^{125}I]PAB at 24 hr. The tumor-to-blood concentration ratios were similar at 1 and 24 hr, but higher with IDAB at 6 hr, due to its faster blood clearance. Tumor-to-muscle concentration ratios were similar at 1 and 6 hr, but higher with [^{125}I]PAB at 24 hr because of its higher tumor concentration. This absolute tumor uptake could possibly be dependent upon the nature of the human melanoma cell line, the specific activity of the tracer used, or to differences in tumor blood flow, tumor volume, necrotic fraction (*24*) or due to high specific binding of the tracer to cell surface receptors and receptor density.

Liver concentration was consistently higher with IDAB than with IPAB by a factor of two or more. This higher liver uptake may be attributed to the higher lipophilicity of IDAB as determined by HPLC retention times. Intestinal activity was higher with IPAB at 1 and 6 hr, but not by 24

TABLE 2
Biodistribution of [^{125}I]PAB and [^{125}I]DAB at One Hour in Nude Mice Xenografted with Human Melanotic Melanoma (%ID/g; mean (s.d.), n = 6)

	[^{125}I]PAB	[^{125}I]DAB	p value
Blood	0.967 (0.168)	1.03 (0.318)	ns
Liver	6.36 (0.770)	12.7 (1.69)	<0.001
Spleen	3.11 (0.789)	3.46 (0.206)	ns
Kidney	3.82 (0.561)	4.63 (0.905)	ns
Bone	0.750 (0.0663)	1.04 (0.476)	ns
Muscle	0.552 (0.0711)	0.988 (0.125)	<0.001
Stomach*	3.23 (0.697)	3.84 (1.98)	ns
Intestine*	10.64 (0.541)	5.04 (1.47)	<0.001
Thyroid	4.23 (0.594)	5.68 (1.02)	0.013
Lung	2.34 (0.277)	6.32 (1.55)	<0.001
Heart	1.14 (0.207)	1.67 (0.210)	0.001
Brain	0.895 (0.0887)	1.04 (0.0855)	0.015
Tumor	3.87 (0.470)	5.18 (1.31)	0.044
Ratio			
Tumor-to-Blood	4.16 (1.09)	5.68 (2.75)	ns
Tumor-to-Muscle	7.16 (1.50)	5.33 (1.65)	ns

*Gastric and intestinal values include their contents.

TABLE 4
Biodistribution of [^{125}I]PAB and [^{125}I]DAB at 24 Hours in Nude Mice Xenografted with Human Melanotic Melanoma (%ID/g; mean (s.d.), n = 6)

	[^{125}I]PAB	[^{125}I]DAB	p value
Blood	0.0617 (0.018)	0.0350 (0.0084)	0.009
Liver	0.263 (0.0216)	1.12 (0.232)	<0.001
Spleen	0.0383 (0.015)	0.0350 (0.023)	ns
Kidney	0.0850 (0.016)	0.065 (0.0197)	ns
Bone	0.0133 (0.0052)	0.0133 (0.0052)	ns
Muscle	0.0117 (0.0041)	0.0150 (0.0084)	ns
Stomach*	0.130 (0.0881)	0.445 (0.386)	ns
Intestine*	0.132 (0.0852)	0.123 (0.0717)	ns
Thyroid	0.100 (0.143)	0.0550 (0.0207)	ns
Lung	0.0717 (0.0075)	0.0633 (0.0273)	ns
Heart	0.0283 (0.0075)	0.0233 (0.0175)	ns
Brain	0.0067 (0.0052)	0.0033 (0.0052)	ns
Tumor	1.028 (0.239)	0.553 (0.241)	0.006
Ratio			
Tumor-to-Blood	17.8 (6.10)	15.5 (4.69)	ns
Tumor-to-muscle	94.5 (32.5)	39.7 (9.61)	0.003

*Gastric and intestinal values include their contents.

hr. Thyroid levels of both agents progressively declined over 24 hr, indicating that in vivo dehalogenation was negligible. Lung activity was initially higher with IDAB, but the differences in distribution in other organs were relatively insignificant.

Images of nude mice with human melanoma xenografts using [^{131}I]PAB and [^{131}I]DAB at 6 hr postinjection showed that both tracers were cleared by the hepatobiliary system (Figs. 3 and 4). Although [^{131}I]DAB demonstrated tumor uptake at 6 hr, there was considerable liver uptake. At 24 hr, as indicated by the biodistribution data, tumor activity cleared and there was still hepatic activity in the body. The tumor was overshadowed by hepatobiliary activity on the 6-hr images with IPAB. However, at 24 hr, the tumor was observed as an area of increased activity. IPAB therefore appears to be a better tracer than IDAB for external imaging human malignant melanoma.

TABLE 3
Biodistribution of [^{125}I]PAB and [^{125}I]DAB at Six Hours in Nude Mice Xenografted with Human Melanotic Melanoma (%ID/g; mean (s.d.), n = 6)

	[^{125}I]PAB	[^{125}I]DAB	p value
Blood	0.208 (0.0542)	0.103 (0.0197)	0.001
Liver	1.16 (0.212)	3.74 (0.427)	<0.001
Spleen	0.330 (0.105)	0.260 (0.0990)	ns
Kidney	0.483 (0.131)	0.435 (0.0909)	ns
Bone	0.115 (0.0236)	0.100 (0.0297)	ns
Muscle	0.0983 (0.0306)	0.0967 (0.0356)	ns
Stomach*	0.757 (0.298)	0.475 (0.164)	ns
Intestine*	2.46 (1.18)	0.423 (0.0963)	0.002
Thyroid	0.583 (0.203)	0.400 (0.124)	ns
Lung	0.387 (0.0568)	0.458 (0.0993)	ns
Heart	0.167 (0.0372)	0.150 (0.0329)	ns
Brain	0.122 (0.0331)	0.132 (0.0204)	ns
Tumor	2.91 (0.463)	2.83 (0.388)	ns
Ratio			
Tumor-to-Blood	14.9 (5.07)	28.1 (5.84)	0.002
Tumor-to-Muscle	32.5 (12.0)	33.3 (14.0)	ns

*Gastric and intestinal values include their contents.

In conclusion, the tracer [^{125}I]PAB was prepared and evaluated as a new malignant melanoma imaging agent. This involved the preparation and characterization of the precursor (2-piperidinylaminoethyl)4-tributyltinbenzamide. The radiolabeled product [^{125}I]PAB was obtained in high yields and with a high specific activity using an iododestannylation reaction. In vitro pharmacological profiles indicated that IPAB had a slightly higher affinity as compared to IDAB for sigma-1 sites and that it binds with high affinity to melanoma cells. Its biodistribution in nude mice bearing human melanoma and imaging of nude mice with [^{131}I]PAB suggested that [^{123}I]PAB is a potential melanoma imaging agent in humans. These results also demonstrate that sigma receptors could be used as external markers for imaging and molecular characterization of tumors using SPECT.

ACKNOWLEDGMENTS

The authors thank Dr. David O. Davis for encouragement and support. We also thank Mr. R.K. Keast for his help with the statistical analysis.

REFERENCES

1. National Institutes of Health Consensus Conference. Diagnosis and treatment of early melanoma. *JAMA* 1992;268:1314–1319.

2. Fawwaz RA, Wang TST, Srivastava SC, et al. Potential of palladium-109 labeled antimelanoma monoclonal antibody for tumor therapy. *J Nucl Med* 1984;25:796–799.
3. Larson SM, Brown JP, Wright PW, Carrasquillo JA, Hellstrom I, Hellstrom KE. Imaging of melanoma with I-131 labeled monoclonal antibodies. *J Nucl Med* 1983;24:123–129.
4. Murray JL, Rosenblum MG, Sobol RE, et al. Radioimmunoimaging in malignant melanoma with ^{111}In-labeled monoclonal antibody 96.5. *Cancer Res* 1985;45:2376–2381.
5. Neumann RD, Cornelius EA, Zoghbi JM, et al. Gallium-67 vs. In-111 DTPA-anti-p97 of In-111-DTPA-anti-p240 murine MoAbs for scintigraphic detection of metastatic melanoma [Abstract]. *J Nucl Med* 1987;28:573.
6. Rosenblum MG, Murray JL, Haynie TP, et al. Pharmacokinetics of ^{111}In-labeled anti-p97 monoclonal antibody in patients with metastatic malignant melanoma. *Cancer Res* 1985;45:2382–2386.
7. Beaumier PL, Krohn KA, Carrasquillo JA, et al. Melanoma localization in nude mice with monoclonal Fab against p97. *J Nucl Med* 1985;26:1172.
8. Taylor A, Milton W, Emre H, et al. Radioimmunodetection of human melanoma with In-111 labeled monoclonal antibody. *J Nucl Med* 1988;29: 329–337.
9. Beierwaltes WH, Varma VM, Counsell RE, Lieberman LM. Scintillation scanning of malignant melanomas with radioresistant quinoline derivatives. *J Lab Clin Med* 1968;72:485.
10. Counsell RE, Pocha P, Ranade VV, Sterngold J, Beierwaltes WH. Tumor localizing agents. VII. Radioiodinated quinoline derivatives. *J Med Chem* 1969;12:232–236.
11. Langevelde A, Bakker CNM, Boer H, et al. Potential radiopharmaceutical for detection of occular melanoma. Part II. Iodoquinoline derivatives and ^{67}Ga citrate. *Eur J Nucl Med* 1986;12:96–104.
12. Lambrecht RM, Packer S, Wolf AP, et al. Detection of occular melanoma with 4-(3-dimethylaminopropylamino)-7[123I] iodoquinoline. *J Nucl Med* 1984;25:800–804.
13. Langevelde A, Bakker CNM, Broxterman HJ, et al. Potential radiopharmaceuticals for the detection of ocular melanoma. Part I. 5-iodo-2-thiouracil derivatives. *Eur J Nucl Med* 1983;8:45.
14. Ichise M, Holman BL, Nagel JS, et al. Demonstration of metastatic melanoma by isopropyl I-125 iodoamphetamine (IMP) [Abstract]. *J Nucl Med* 1986;27:971.
15. Cohen MB, et al. Detection of malignant melanoma with I-123 iodoamphetamine. *J Nucl Med* 1988;29:1200–1206.
16. Michelot JM, Moreau MC, Labarre PG, et al. Synthesis and evaluation of new iodine-125 radiopharmaceuticals as potential tracers for malignant melanoma. *J Nucl Med* 1991;32:1573–1580.
17. Michelot J, Bonafus J, Veyre A, et al. Preliminary clinical evaluation of iodine-123-N-(2-diethylaminoethyl)4-iodobenzamide in the detection of malignant melanoma (MM) and metastases [Abstract]. *Eur J Nucl Med* 1990; 17:S66.
18. John CS, Saga T, Kinuya S, et al. An improved synthesis of [^{125}I]N-(2-diethylaminoethyl)4-iodobenzamide: a potential ligand for imaging malignant melanoma. *Nucl Med Biol* 1993;20:75–79.
19. John CS, Saga T, et al. Preparation and characterization of [I-125]PAB: a potential malignant melanoma imaging radiopharmaceutical [Abstract]. *J Nucl Med* 1992;33:889.
20. Todaro GJ, Fryling C, De Larco JE. Transforming growth factors produced by certain human tumor cells: polypeptides that interact with epidermal growth factor receptors. *Proc Natl Acad Sci USA* 1980;77:5258–5262.
21. Clanton JA, de Paulis T, Schmidt DE, et al. Preparation of [^{123}I]- and [^{125}I]epidepride: a dopamine D-2 receptor antagonist radioligand. *J Lab Compd Radiopharm* 1991;29:745–751.
22. Walker JM, Bowen WD, Walker FO, Matsumoto RR, de Costa BR, Rice KC. Sigma receptors: biology and function. *Pharmacol Rev* 1990;42:355–402.
23. Vilner BJ, Bowen WD. Characterization of sigma-like binding sites of NB41A3, S-20Y, and N1E-115 neuroblastomas, C6 glioma, and NG108-15 neuroblastoma-glioma hybrid cells: further evidence for sigma-2 receptors. In: Kamenka J-M, Domino EF, eds. *Multiple sigma and PCP receptor ligands*. Ann Arbor, MI: NPP Books; 1992:341–353.
24. Lyng H, Skretting A, Rofstad EK. Blood flow in six human melanoma xenograft lines with different growth characteristics. *Cancer Res* 1992;52: 584–592.